Automated Lane Change Controller Design

Cem Hatipoglu, *Member, IEEE*, Ümit Özgüner, *Member, IEEE*, and Keith A. Redmill, *Member, IEEE*

***Abstract*—The primary focus of study in this paper is the background control theory for automated lane change maneuvers. We provide an analytic approach for the systematic development of controllers that will cause an autonomous vehicle to accomplish a smooth lane change suitable for use in an Automated Highway System. The design is motivated by the discontinuous availability of valid preview data from the sensing systems during lane-to-lane transitions. The task is accomplished by the generation of a virtual yaw reference and the utilization of a robust switching controller to generate steering commands that cause the vehicle to track that reference. In this way, the open loop lane change problem is converted into an equivalent virtual reference trajectory tracking problem. The approach considers optimality in elapsed time at an operating longitudinal velocity. Although the analysis is performed assuming that the road is straight, the generalization of the proposed algorithm to arbitrary road segments is rather straightforward. The outlined lane change algorithm has been implemented and tested on The Ohio State University test vehicles. Some of the experimental results are presented at the conclusion of this paper.**

***Index Terms*—Automated highways, automated vehicles, lane change maneuvers, mobile robots.**

I. Introduction

AN AUTONOMOUS vehicle is required to perform two partially decoupled tasks simultaneously, i.e., 1) to adjust its speed so as to maintain headway safety and 2) to steer so as to control the lateral motions of the vehicle. Having made this classification, we note here that the focus of this paper will be the lateral control issue and, more specifically, automated lane change maneuvers.

On multiple lane highways, a lane change capability would provide more flexibility, but also more tasks to a supervisory controller. Two low-level controllers, which are used to achieve the autonomous "lane keeping" and "lane changing" tasks, are needed to cover all the requirements of an advanced decision-making mechanism in a hierarchical structure [12]. The "lane keeping" algorithm used in The Ohio State University (OSU) vehicles has been presented in [9]. In this paper, a time optimal lane change algorithm with absolute bounds on some states will be studied. Young and Özgüner [17] have previously examined an optimal automatic steering control with fixed terminal constraints, which is based on an elegant time varying sliding manifold design approach. However, discontinuous availability of certain states during the transition makes it impossible to realize this controller within our framework without major modifications to sensors or road infrastructure. Tan *et al.* [15] reported results on lane change maneuvers for look-down systems that primarily focused on two schemes: infrastructure guided lane changes and lane changes with dead reckoning. The former corresponds to the situation in which lateral position information is made continuously available to the controller by means of infrastructure enhancements, specifically the installation of extra magnets to mark a path between adjacent lanes. The latter is similar in concept to the case studied in this paper, in which a sensory "dead-zone" period is encountered during the lane transition. Rajamani *et al.* summarize the theoretical reasoning behind the PATH program's lane changing controller and present the experimental results obtained in San Diego, CA, in [18] along with some practical insights. A similar situation with continuously available data is examined by Kato *et al.* [10] to generate transition paths so as to accomplish smooth lane changes with a vision system.

This paper summarizes the development and experimental validation of the lane change controller designed for the OSU test vehicles that participated in the 1997 National Automated Highway System Consortium (NAHSC) demonstration in San Diego, CA. The design is based on a look-ahead system that has dead-reckoning requirements (due to sensory system limitations) during the transitional period from one lane to another. This constraint, combined with passenger comfort criterion during the maneuver, converts the existing problem into a time optimal control problem with inequality type constraints on the system states. The lane change controller design problem is simplified by employing an intelligent cruise control system that maintains constant vehicle speed during the lane change maneuver. This allows one to decouple the longitudinal dynamics entirely in the design and to work with a linear bicycle model (actually a nonlinear model operating at a constant speed). The methodology generates a reference jerk signal that yields the time optimal trajectory while satisfying upper bounds on lateral acceleration and jerk. This signal is used to determine the yaw rate and yaw angle references, which are then integrated with an internal sliding mode controller to achieve the lane changing goal while providing robustness against uncertainties in the model parameters and bounded disturbances. Finally, the lane change controller is blended with the lane keeping controller to provide comfortable transitions between different lateral control modes.

In any application-oriented design, the motivation behind the design path pursued lies in the plant to be controlled and the available sensors and actuators. Modularity and flexibility are always desirable, but the controller must work on the system

Manuscript received March 6, 2000; revised February 17, 2003. This work was supported by The Ohio State University Center for Intelligent Transportation Research and by Honda Research and Development. The Associate Editor for this paper was A. Broggi.

C. Hatipoglu is with Honeywell Bendix Commercial Vehicle Systems, Elyria, OH 44035 USA (e-mail: cem.hatipoglu@bendix.com).

Ü. Özgüner and K. A. Redmill are with the Department of Electrical Engineering, The Ohio State University, Columbus, OH 43210-1272 USA (e-mail: umit@ee.eng.ohio-state.edu; redmill@ee.eng.ohio-state.edu).

Digital Object Identifier 10.1109/TITS.2003.811644

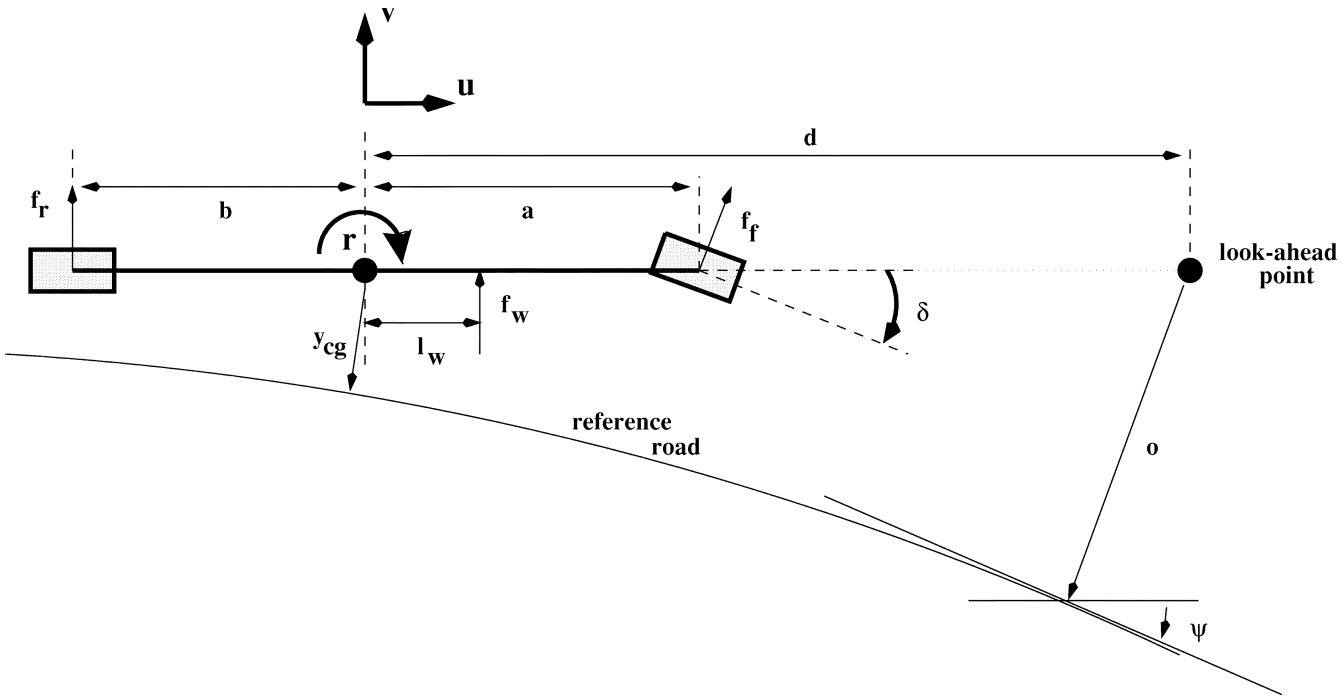

Fig. 1. Bicycle model for a vehicle.

in hand. Therefore, moving from the "general concept" to a "particular case" becomes unavoidable. In this case, the choice of a design procedure was mandated by the fact that preview sensor information (which is used in our lane-keeping algorithm) cannot be measured continuously during the transition from one lane to another using either the vision or the radar reflective sensors. There is a dead-zone period when the preview information sensing systems do not provide useful data. This creates a transition period that must be handled "open loop" with respect to lateral position information. Attempts to generate a true open-loop time series steering angle command profile fail because of wind and super-elevation disturbances, nonsmooth actuator nonlinearities, unmodeled vehicle–road interactions, and uncertainties in the (possibly time varying) plant parameters. Most of these dynamics and disturbances can be bypassed through yaw rate measurement so for the lane change a vehicle yaw rate controller was designed and used to implement a desired time series yaw rate profile, that would bring the vehicle to the center of the next lane and preserve the vehicle's angular alignment with the road.

The organization of this paper is as follows. First, a model of the vehicle, sensor, and actuator assembly will be presented. The lane change control design procedure will then be given in detail, followed by some experimental results.

II. Vehicle Model

It is assumed that the vehicle is operating on a flat surface and that a linearized bicycle model is capable of describing the motion of the vehicle effectively. The standard linearizing small angle assumptions are made for the tire slip angles and the front tire steering angle. A wind disturbance is modeled that affects the lateral and yaw motions of the vehicle. The corresponding model is depicted in Fig. 1. The variables represent the following physical quantities: $u(t)$, $v(t)$, and $r(t)$ are the longitudinal velocity (in meters per second), lateral velocity (in meters per second) and the yaw rate (in radians per second) respectively, $\delta(t)$ is the actual steering angle of the front tires (positive for clockwise turn) (in radians), $\psi(t)$ is the yaw angle with respect to the road (in radians), $y_{\rm cg}(t)$ is the deviation of the vehicle's center of gravity from the lane center (in meters), $o(t)$ is the offset signal at the look-ahead distance (in meters), f_f and f_r are the lateral tire forces on the front and rear tires, respectively (in Newtons per radian), a and b are the distances from the center of gravity of the vehicle to the front and rear axles, respectively (in meters), l_w is the position (in meters) at which a wind disturbance force of f_w (in Newtons) laterally affects the vehicle motion, d is the sensor preview distance (in meters), and $\rho(t)$ is the road curvature at the look-ahead point (in 1/m).

A. Vehicle Dynamics

Assuming that there is a longitudinal controller engaged to keep the vehicle speed (u) constant, the vehicle dynamics considered in this paper are represented by the following set of linear system equations [4], [5], [7]:

$$\dot{v}(t) = a_{11}v(t) + a_{12}r(t) + b_1\delta(t) + d_1 f_w \tag{1a}$$
$$\dot{r}(t) = a_{21}v(t) + a_{22}r(t) + b_2\delta(t) + d_2 f_w \tag{1b}$$
$$\dot{y}_{\rm cg}(t) = v(t) + u\psi(t) \tag{1c}$$
$$\dot{\psi}(t) = u\rho(t - t_o) - r(t) \tag{1d}$$
$$\ddot{z}(t) = u^2\big[\rho(t) - \rho(t - t_o)\big] - du\dot{\rho}(t - t_o) \tag{1e}$$
$$o(t) = y_{\rm cg}(t) + d\psi(t) + z(t) \tag{1f}$$

where $z(t)$ is a dummy variable that is necessary to characterize the transient response of the offset signal precisely. In this context, $o(t)$ is the measured offset from lane center at the

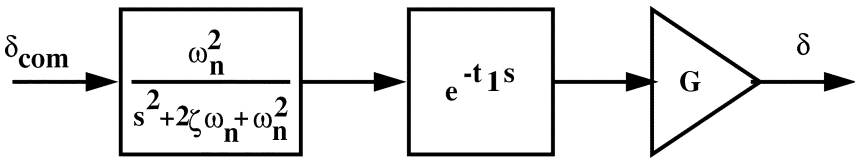

Fig. 2. Steering actuator model block diagram.

look-ahead point (positive to the left of the lane center) and the lateral position of the vehicle center of gravity $y_{\rm cg}(t)$ (also positive to the left of the lane center) is to be regulated to zero for all possible road curvature reference inputs $\rho(t)$ (positive for clockwise turns) defining the desired path to be followed using the front wheel steering angle $\delta(t)$ (positive for clockwise turns). The linearized model is valid at the operating longitudinal velocity u (positive for forward motion), which is assumed to be held constant by means of a decoupled longitudinal controller, and for small values of $\rho(t)$. The sensor delay t_o depends on the operating velocity and the preview distance d and is given by $t_o = d/u$. The other parameters of the vehicle model (1) are determined from

$$\begin{aligned} a_{11} &= -\frac{k_f + k_r}{mu} \\ a_{12} &= u + \frac{ak_f - bk_r}{mu} \\ b_1 &= -\frac{k_f}{m} \\ a_{21} &= \frac{ak_f - bk_r}{uI_z} \\ a_{22} &= -\frac{a^2k_f + b^2k_r}{uI_z} \\ b_2 &= \frac{ak_f}{I_z} \\ d_1 &= \frac{1}{m} \\ d_2 &= -\frac{l_w}{I_z} \end{aligned}$$

where $k_f > 0$ and $k_r > 0$ are the lateral tire stiffness coefficients of the front and rear tires, respectively, m is the (virtual) mass of the vehicle, and I_z is the (virtual) moment of inertia around the center of mass perpendicular to the plane in which the vehicle is located. The remaining variables are as previously defined.

The derivative of the road curvature can be eliminated by simple algebraic manipulations and straightforward substitutions, which lead to the following alternative set of equations for (1c)–(1f):

$$\begin{aligned} \ddot{y}_{\rm cg}(t) &= a_{11}v(t) + (a_{12} - u)r(t) + b_1\delta(t) + d_1 f_w \\ &\quad + u^2\rho(t - t_o) \qquad (2a) \\ \ddot{\phi}(t) &= (a_{11} - da_{21})v(t) + (a_{12} - da_{22} - u)r(t) \\ &\quad + (b_1 - db_2)\delta(t) + (d_1 - dd_2)f_w + u^2\rho(t). \qquad (2b) \end{aligned}$$

B. Actuator Dynamics

The steering actuator assembly consists of a dc motor, worm-gear drive, and a low-level reference tracking controller. The motor itself is installed on the steering rack and is also used to provide driver-assist power steering. Due to the coulomb friction-type nonlinearities within the assembly, the actuation process contains a pure delay term, which appears to decrease at higher speeds as the frictional load force stemming from the tire–road interaction becomes smaller. The overall assembly is observed to be effectively represented by a pure delay term cascaded with a second-order linear system, as shown in Fig. 2, and is modeled as

$$H(s) = G \cdot \frac{\omega_n^2}{s^2 + 2\zeta\omega_n + \omega_n^2} e^{-t_1 s} \qquad (3)$$

where the actuator delay t_1, which is approximately constant in the 45–60-mi/h range, natural frequency ω_n, and damping coefficient ζ are determined experimentally. The gain G, which includes the gear ratios, is known to be 1/19160. The magnitude of the delay term and the second-order system coefficients were obtained from open-loop tests performed on a flat asphalt test track.

Typical parameters approximating those of the OSU vehicles are given in Table I.

TABLE I
TYPICAL MODEL PARAMETERS FOR THE OSU VEHICLES

a	1.35 m	cg to front axle distance
b	1.37 m	cg to rear axle distance
m	1569 kg	total mass of the vehicle
k_f	5.96×10^4 $\frac{\rm N}{\rm rad}$	cornering stiffness (front)
k_r	8.66×10^4 $\frac{\rm N}{\rm rad}$	cornering stiffness (rear)
I_z	272.4 Ns/rad	moment of inertia
u	$[1, 40]$ m/s	range of longitudinal speed
d	8.1 m	preview distance
G	1/19160	actuator gain
ω_n	22.94 rad/s	actuator natural frequency
ζ	0.517	damping coefficient
t_1	0.03 s	actuator delay

III. LANE CHANGE CONTROLLER DEVELOPMENT

A. Open Loop Lane Change Problem

The lane change problem can be summarized as follows: while maintaining lane keeping at a longitudinal speed u, the vehicle travels a specified distance (a full lane width) along the lateral axis with respect to its body orientation within a finite time period and aligns itself with the adjacent lane at the end of the maneuver such that the lane keeping task can be resumed safely and smoothly. The autonomous lane change problem deals with the generation of the appropriate steering signal to cause the vehicle to accomplish the above-described task without driver assistance. The major design assumptions are: 1) only the yaw rate r and the steering angle δ are measured;

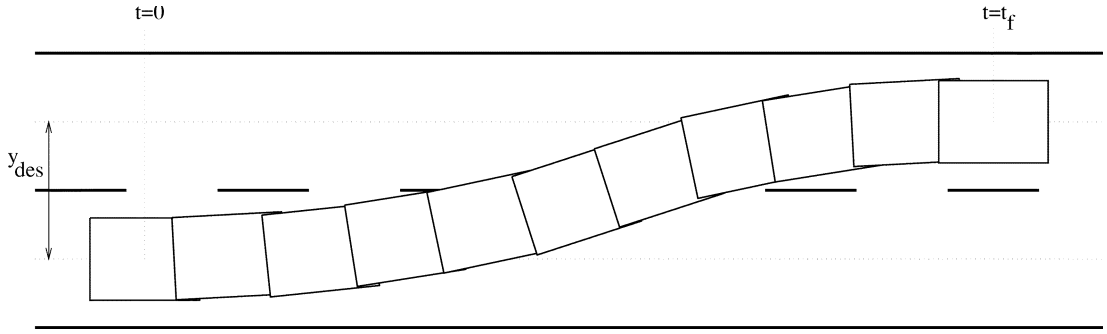

Fig. 3. Lane change maneuver.

2) vehicle parameters are known within a bounded neighborhood of some nominal values; and 3) the road curvature does not change significantly during the lane change maneuver.

B. Simplified Mathematical Interpretation

Consider the simplified sub-model

$$\dot{y}_{\rm cg} = v_{\rm cg} \tag{4a}$$
$$\dot{v}_{\rm cg} = a_{\rm cg} \tag{4b}$$
$$\dot{a}_{\rm cg} = J_{\rm cg} = \tilde{\delta} \tag{4c}$$

where $y_{\rm cg}(0) = v_{\rm cg}(0) = a_{\rm cg}(0) = 0$ defines ideal tracking of a straight road segment with $y_{\rm cg}$ denoting the lateral position of the vehicle center of gravity with respect to the original lane center. At the end of the maneuver, with $t = t_f$, $v_{\rm cg}(t_f) = a_{\rm cg}(t_f) = 0$ is required and $y_{\rm cg}(t_f) = y_{\rm ref}$ should also be achieved. This is illustrated in Fig. 3. For the moment, assume the time-optimal control problem with a bound on lateral jerk where optimality in time refers to the minimization of maneuver time with fixed end constraints. For this system, the Hamiltonian can be written as $\mathcal{H} = 1 + p_1 v_{\rm cg} + p_2 a_{\rm cg} + p_3 \tilde{\delta}$ from which the co-states are obtained as follows:

$$\begin{aligned}
\dot{p}_1 &= -\frac{\partial \mathcal{H}}{\partial y_{\rm cg}} = 0 \Rightarrow p_1(t) = p_{10} \\
\dot{p}_2 &= -\frac{\partial \mathcal{H}}{\partial v_{\rm cg}} = -p_1 \Rightarrow p_2(t) = -p_{10}t + p_{20} \\
\dot{p}_3 &= -\frac{\partial \mathcal{H}}{\partial a_{\rm cg}} = -p_2 \Rightarrow p_3(t) = \frac{p_1 0}{2}t^2 - p_{20}t + p_{30}.
\end{aligned} \tag{5}$$

The control law that minimizes the Hamiltonian is given by

$$\tilde{\delta} = -|J_{\max}| \cdot \mathrm{Sign}\big(p_3(t)\big). \tag{6}$$

Since $p_3(t)$ is a second-order polynomial, $\tilde{\delta}$ can change sign at most twice. If we assume that $\tilde{\delta}$ does not change sign in the time interval $t \in (0, t_f]$, then $\tilde{\delta} = \pm|J_{\max}| \neq 0$ continuously, which means $a_{\rm cg}(t_f) = \pm|J_{\max}|t_f \neq 0$ for any nonzero $J_{\max}$. Therefore, $\tilde{\delta}$ must change sign at least once. If we assume that it changes sign only once at $t = t_1$, then t_1 has to be equal to $t_f/2$ to achieve $a_{\rm cg}(t_f) = 0$. However, then $v_{\rm cg}(t_f) = \pm|J_{\max}|(t_f/2)^2 \neq 0$. Since $\tilde{\delta}$ must change sign more than once and at most twice, we conclude that $\tilde{\delta}$ switches between $\pm|J_{\max}|$ exactly twice in the time interval $t \in (0, t_f]$.

This analysis corresponds to bounded-input time-optimal control design. However, lateral acceleration should be absolutely bounded as well. With the inequality constraints on the state $a_{\rm cg}(t)$ as well as the control input $\tilde{\delta}$, the time-optimal control does not exist in the class of piece-wise continuous functions. When the state $a_{\rm cg}$ reaches its upper bound there are high-frequency switchings between $\pm|J_{\max}|$ such that the mean value of $a_{\rm cg}$ remains on the boundary. The equivalent control applied during that interval is zero. Therefore, the most generalized time-optimal control signal that satisfies the bounds on the lateral acceleration as well as the lateral jerk is as shown in Fig. 4.

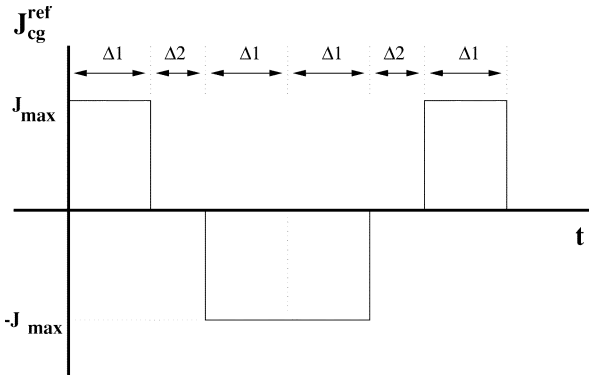

Fig. 4. Time optimal lateral jerk reference signal.

The condition on the final value of $y_{\rm cg}$ yields

$$\begin{aligned}
y_{\rm des} &= \int\int\int J_{\rm cg}^{\rm ref}(\tau)\, d\tau\, d\alpha\, d\beta \\
&= \Delta_1 \left(2\Delta_1^2 + 3\Delta_1\Delta_2 + \Delta_2^2\right) J_{\max}.
\end{aligned} \tag{7}$$

This equation must be solved for Δ_1 and Δ_2 given the desired lateral displacement $y_{\rm ref}$ and the absolute bounds on the lateral acceleration $A_{\max}$ and jerk $J_{\max}$. The solution procedure is as follows. First, find Δ_1 from

$$\Delta_1 = \min\left\{\frac{A_{\max}}{J_{\max}}, \sqrt[3]{\left|\frac{y_{\rm des}}{2J_{\max}}\right|}\right\}. \tag{8}$$

Δ_2 is then the minimum real positive root of Δ_2 found from solving (7), or zero if there are no positive real roots.

C. Generation of Reference Signals

The previous section provides the ideal lateral jerk, acceleration, velocity, and displacement signals that the vehicle's center of gravity should follow to perform a lane change maneuver while preserving passenger comfort. However, the only input to the vehicle is commanded steering angle. Therefore,

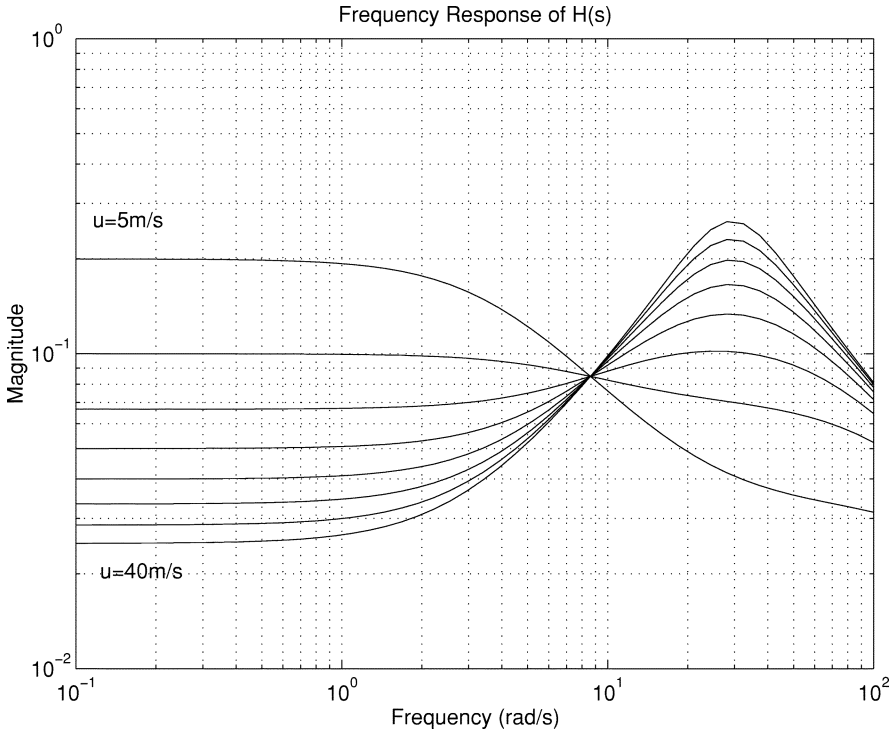

Fig. 5. Magnitude plot of lateral jerk to yaw angle $H(s)$.

these results must ultimately be used to generate steering angle commands. This can be accomplished by generating a reference yaw rate signal and applying a yaw rate controller to generate steering angle commands.

From the vehicle model, we can obtain lateral velocity and yaw rate transfer functions of the form

$$\frac{v(s)}{\delta s} = \frac{q_1(s)}{p(s)} \tag{9}$$

$$\frac{r(s)}{\delta s} = \frac{q_2(s)}{p(s)} \tag{10}$$

where

$$q_1(s) = b_1 s + (a_{12}b_2 - a_{22}b_1) \tag{11a}$$

$$q_2(s) = b_2 s + (a_{21}b_1 - a_{11}b_2) \tag{11b}$$

$$p(s) = s^2 - (a_{11} + a_{22})s + a_{11}a_{22} - a_{12}a_{21}. \tag{11c}$$

Under the assumptions that $f_w = 0$, which implies that the vehicle is operating on a straight road segment, and that the necessary steering angle remains small, straightforward algebraic manipulations yield

$$r(s) = \frac{q_2(s)}{a_{11}q_1(s) + (a_{12} - u)q_2(s) + b_1 p(s)} \cdot \frac{J_{\text{cg}}(s)}{s} \tag{12}$$

since [from (1c)] v_{cg} can be approximated as $v_{\text{cg}}(t) \approx v(t) - u\int_0^t r(\tau)d\tau$. Equation (12) provides an important equality since it relates the lateral jerk signal to the yaw rate signal. The vehicle is equipped with a yaw rate sensor, so by using the ideal jerk signal (shown in Fig. 4) in (12) a reference yaw rate signal can be derived, which can be achieved within a feedback control scheme.

It is useful to study the frequency response of the transfer function $H(s) = sr(s)/J_{\text{cg}}(s)$ at various longitudinal velocities. $|H(s)|$ is plotted for $u = [5, \ldots, 40]$ m/s with 5-m/s increments in Fig. 5. One noteworthy observation is that the dc gain of $|H(s)|$ is $1/u$ and that the frequency response is relatively flat over a wide range of velocities in the domain of lower frequencies. This observation allows further simplifications, especially during implementation stages.

The reference yaw rate and yaw angle signals can be determined from the idealized lateral jerk signal $J_{\text{cg}}^{\text{ref}}$ using

$$r_{\text{cg}}^{\text{ref}}(s) = H(s)\frac{J_{\text{cg}}^{\text{ref}}(s)}{s} \tag{13}$$

$$\psi_{\text{cg}}^{\text{ref}}(s) = H(s)\frac{J_{\text{cg}}^{\text{ref}}(s)}{s^2} \tag{14}$$

which can be approximated as

$$r_{\text{cg}}^{\text{ref}}(t) = \frac{1}{u}\int_0^t J_{\text{cg}}^{\text{ref}}(\tau)d\tau \tag{15}$$

$$\psi_{\text{cg}}^{\text{ref}}(t) = \frac{1}{u}\int_0^t \int_0^\beta J_{\text{cg}}^{\text{ref}}(\tau)d\tau d\beta \tag{16}$$

assuming that the high-frequency dynamics of $H(s)$ are not excited by the choice of the reference jerk signal. This is observed to be the case experimentally. The bounds $J_{\max}$ and $A_{\max}$ prevent the maneuver from occurring too quickly. Typically, in a nonemergency situation, the lane change will be accomplished in 5–6 s. A faster lane change can create unsettling motions for passengers. Hence, the major frequency component will be in the 1.2–1.0-rad/s range during the transition. When Fig. 5 is examined, it is clear that the magnitude of $H(s)$ around these frequencies is essentially the same as the dc gain for almost all longitudinal velocities. This analysis, along with experimental

studies, justifies the validity of the approximation. However, this result could be extended by implementing a speed-dependent $H(s)$, filtering the input signal, obtaining the required reference signals without approximation, and using them to generate a yaw rate command profile.

D. Sliding Mode Yaw Rate Follower

Let $\psi(t) = \int_0^t r(\tau)d\tau$ be the yaw angle of the vehicle. Also let $\psi_d(t) = \int_0^t r_{\rm cg}^{\rm ref}(\tau)d\tau$ be the desired yaw angle. Given $\epsilon_\psi = \psi - \psi_d$ and $\dot{\epsilon}_\psi = \dot{\psi} - \dot{\psi}_d = r - r_{\rm cg}^{\rm ref}$, define the conventional sliding manifold as

$$S = \dot{\epsilon}_\psi + \mu\epsilon_\psi \tag{17}$$

for some positive μ, which determines the convergence rate to the origin when the sliding mode occurs. Specifically, in the sliding mode (i.e., when $S = 0$), ϵ_ψ will decay exponentially to zero yielding $\psi \to \psi_{\rm cg}^{\rm ref}$ and $r \to r_{\rm cg}^{\rm ref}$ if $S \cdot \dot{S} < 0$ can be attained with discontinuous control. To investigate the conditions to achieve sliding mode, consider $\dot{S} = 0$, where

$$\begin{aligned}\dot{S} &= \dot{r} - \dot{r}_{\rm cg}^{\rm ref} + \mu r - \mu r_{\rm cg}^{\rm ref} \\ &= a_{21}v + (a_{22}+\mu)r + d_2 f_w - \frac{J_{\rm cg}^{\rm ref} + \mu A_{\rm cg}^{\rm ref}}{u} + b_2\delta. \end{aligned} \tag{18}$$

For the moment, assume that the tire steering angle can be assigned discontinuous values. The switching control law $\delta = -(M/b_2)\mathrm{Sign}(S)$ with the constraint (since $b_2 > 0$)

$$M > |a_{21}v| + |(a_{22}+\mu)r| + |d_2 f_w| + \frac{J_{\max} + \mu A_{\max}}{u} \tag{19}$$

would guarantee $\dot{S} \cdot S < 0$ and, hence, the existence of the sliding mode. However, note that, due to actuation limits, the discontinuous steering angle cannot be achieved at the wheels. Therefore, we define another layer of (a biased fictitious) sliding manifold $(\tilde{S})$ as

$$\tilde{S} = \delta + \frac{M}{b_2}\mathrm{Sign}(S) \tag{20}$$

and replace the discontinuous function with a continuous approximation such as $\mathrm{Sign}(S) \to 2\tan^{-1}(kS)/\pi$, where $k \in \mathbb{N}$ is the approximation order. If the actual steering command signal $(\delta_{\rm com})$ is chosen according to this law, then

$$\dot{\delta}_{\rm com} = -\tilde{M}\mathrm{Sign}(\tilde{S}) \tag{21}$$

where $\tilde{S}$ is calculated from $\tilde{S} = G\delta_{\rm com} + (M/b_2)\mathrm{Sign}(S)$ with $\tilde{M}$ being the maximum angular rate of the steering actuator and G being the steering actuator gain, then it is possible to achieve adequate suppression of uncertainties and external disturbances. Since the delay term ($\approx$0.36 s) in the actuation system is small compared to the overall duration of the maneuver ($\approx$6 s) at the controller update frequency of 100 Hz, it can be neglected. The above analysis also assumes that the actuator dynamics, as given in (3), can be approximated by a first-order system in the frequency domain of interest, which is experimentally shown to be valid up to approximately 1.25 rad/s.

TABLE II
TYPICAL LANE CHANGE CONTROLLER PARAMETER VALUES

J_{max}	0.067*g m/s^3	maximum admissible lateral jerk
A_{max}	0.067*g m/s^2	maximum admissible lateral acceleration
u	[1..30] m/s	operating longitudinal velocity
u	$[45, \cdots, 65]$ MPH	range of longitudinal speed
γ	0.1	continuous approximation parameter
y_{des}	4 m	lane width

The final controller is implemented using a continuous approximation of the switching term

$$\dot{\delta}_{\rm com} = -\tilde{M}\frac{\tilde{S}}{\sqrt{\tilde{S}^2 + \gamma^2}}. \tag{22}$$

The parameter values used for highway driving are given in Table II.

E. Smooth Switching

The proposed lane change control strategy assumes that the road remains straight during the entire duration of the maneuver. Although the switching controller provides robustness against some of the unmodeled dynamics and external disturbances, there is virtually no compensation for variations in the road curvature. Should the actual road reference be different than the virtual road reference, the lane change maneuver is likely to end with the vehicle offset from the new lane center (undershoot or overshoot depending on the direction of curvature) and possibly with an orientation error. If the road curvature is not too great, the resulting deviation can be corrected by the lane keeping controller. As soon as the lane change maneuver is completed, the lane keeping algorithm is resumed. However, the primary objective of the lane keeping controller is to maintain the vehicle at the lane center and, therefore, if the lane change maneuver ends with a noticeable offset error, a substantial jerk may occur as the position error is corrected. To avoid an uncomfortable or severe jerk, a time-varying gain scheduling on the offset signal is applied within a finite-time window following the switching from lane changing to lane keeping mode. We use a saturation nonlinearity that linearly increases from 0.0 to 1.0 within ΔT s following the controller switching. This nonlinearity scales the measured offset signal. ΔT is determined from the worst admissible scenario considering the frequency response of the steering actuator and taken to be 5 s.

F. Further Generalization of the Algorithm

This control law is designed for use on straight road segments. However, the generated yaw rate and yaw angle signals can be considered as additive terms to the yaw rate necessary to keep the vehicle in the lane center. If the curvature of the road is known to a certain extent, it is possible to derive the required yaw rate to follow the curve from the steady-state equality $r = u\rho$. There are means of estimating the road curvature by fitting curves to vision or radar data or simply by appropriate filtering of the yaw sensor output while the vehicle is in lane keeping. Incorporating this information into the control algorithm, the most restrictive assumption becomes: (3) that

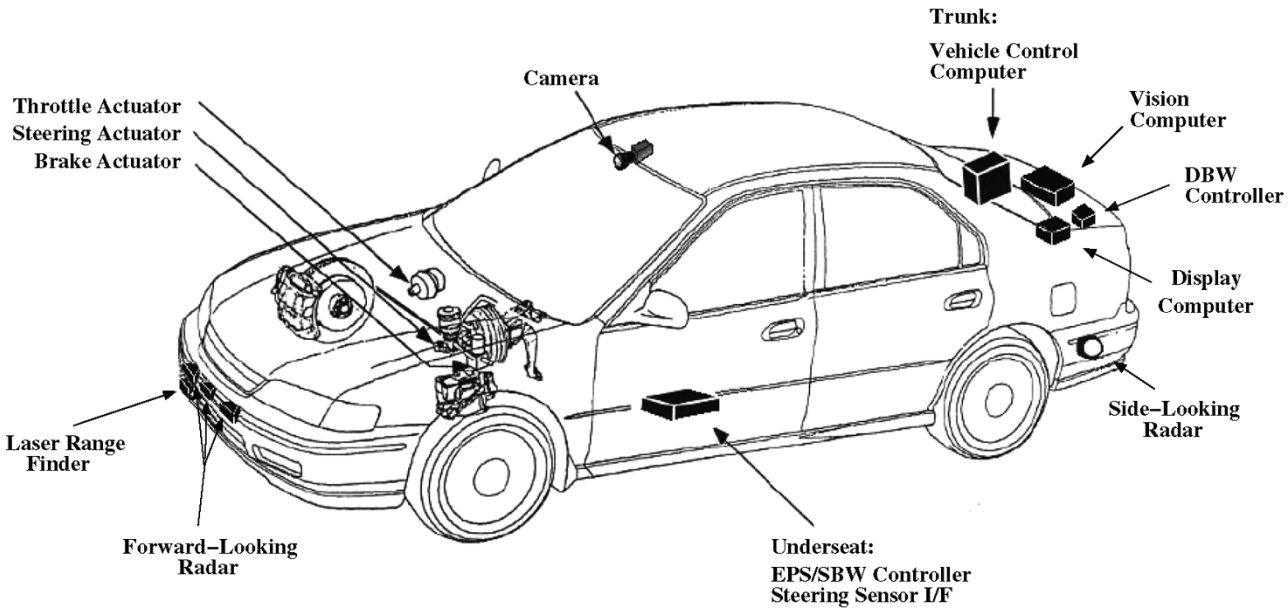

Fig. 6. OSU autonomous vehicle layout.

the road curvature must remain almost constant during the entire lane change maneuver. Since optimality in elapsed time is considered, the maneuver will take a short period of time. Hence, this assumption will not be violated significantly on highways. A Kalman observer designed to use r, u, and δ to estimate the low-pass filtered version of r/u provides a good estimate of the road curvature, and with the assumption that road curvature remains constant throughout the lane change maneuver (approximately 6 s) a lane change can be performed on curved roads by appropriately modifying (15) and (16) to obtain

$$r_{\rm cg}^{\rm ref}(t) = u\rho_s + \frac{1}{u}\int_0^t J_{\rm cg}^{\rm ref}(\tau)d\tau \tag{23}$$

$$\psi_{\rm cg}^{\rm ref}(t) = u\rho_s t + \frac{1}{u}\int_0^t\int_0^\beta J_{\rm cg}^{\rm ref}(\tau)d\tau d\beta \tag{24}$$

where ρ_s is the estimated road curvature at the start of the maneuver.

IV. Vehicle Overview

The cars used in our experiments and demonstrations were modified 1996 Honda Accord LX's. The vehicles were provided by Honda Research and Development and had steer by wire (SBW) and drive by wire (DBW) throttle and brake control capabilities, as well as access to a number of vehicle state measurements.

A. Lateral Control Actuators and ECUs

The factory-installed hydraulic power-steering system was replaced with an electric power-steering assembly consisting of a motor with a worm drive and an absolute rotary position encoder mounted directly under the steering rack of the vehicle. This system provides both driver assist power steering when the vehicle is in manual mode and computer-controlled steering. Two steering Electronic Control Units (ECUs) were provided, one that handles the driver-assist power steering and one that handles computer-controlled steering. Data communication between the control computer and the SBW ECU occurs across an RS-422 serial link. Torque and current sensors in the steering system can disengage automated steering if the driver attempts to steer the vehicle manually or if a failure occurs in the steering actuator, position sensor, or ECU. Each ECU also performs a diagnostic self-check of itself and its associated actuators and sensors at engine start.

B. Physical Layout of Vehicle Hardware

Fig. 6 shows the physical layout of the equipment in the vehicle. The steering ECUs are mounted under the front of the drivers seat. The location of the video camera (replacing the central rear-view mirror), radar RF components (behind the front bumper shroud), and the steering actuator are indicated. The contents of the trunk, including the image-processing computer, vehicle control computer, graphical status display computer, angular rate gyro, radar signal processing components, and interface electronics are also shown.

C. Radar Reflective Stripe Sensor

The radar sensor measures lateral position by sensing backscattered energy from a frequency-selective surface constructed as lane striping and mounted in the center of the lane. The radar reflective surface is designed such that radar energy at a particular frequency is reflected back toward the transmitting antenna at a specific elevation angle. Thus, by varying the frequency of the radar signal, we can vary the look-ahead distance of the sensor. The radar chirps between 10–11 GHz over a 5-ms period, transmitting the radar signal from a centrally located antenna cone. Two receiver cones, separated by approximately 14 in, receive the reflected radar energy. The received signal from each antenna cone is down-converted into the audio range by mixing with the transmit signal, and the relative signal

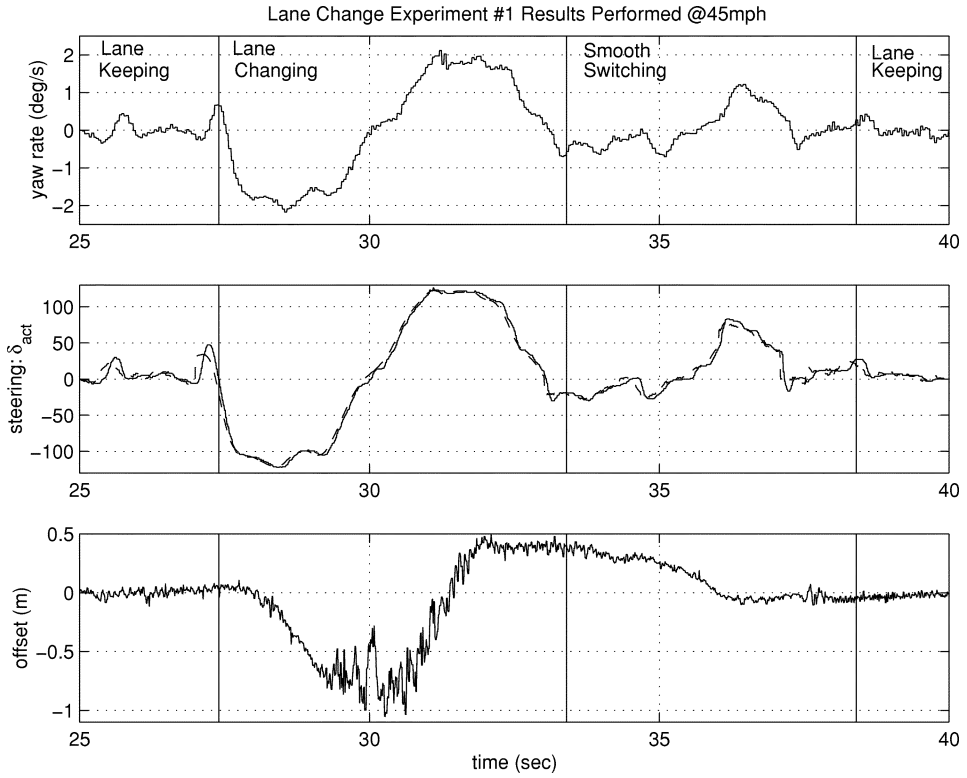

Fig. 7. Experimental results: a left lane change maneuver.

strengths are used to determine the offset distance measurement. In addition, the peak energy in the down-converted signal appears at a frequency that is a function of the distance from the vehicle to an object ahead. It is thus possible to extract the distance to an object ahead of the automated vehicle using the radar hardware already in place for lateral sensing. Finally, by analyzing the signature of the received signal, it is possible to determine whether the stripe is dry, wet, or covered with snow or oil. The radar system's on-vehicle accuracy is ± 5 cm at a look-ahead distance of approximately 5 m. The measurement update rate corresponds to the chirp rate, in this case 200 Hz. Final signal processing of the radar data was done on a small single-board computer and the results transmitted to the control computer over an RS-232 serial interface at a rate of 100 Hz.

A complete description of the radar system can be found in [6].

D. Vision-Based Lane Position Sensor

An image-processing algorithm was developed to extract lane marker information from monochrome single camera image data in a form suitable for automated steering. It assumes a flat dark roadway with light colored lane markers, either solid or broken, painted on it. The algorithm is based on extracting statistically significant *bright* regions from the image plane using a matched filter, and fitting functions to those points that are consistent with the qualitative properties of roadway lanes and ground to image plane geometric relationships and perspective transformations. Historical information about lane markers located in previous image frames is used to predict the location of lane markers in the current image. An estimate of the location of the virtual center line of the lane is formed using left and right lane marker information if both are available, otherwise a virtual center line is formed from the visible lane marker and an estimate of the lane width, and a low-order polynomial is fitted to the discrete location estimates. Position information needed for steering control is extracted from the equation for this virtual center line.

Images are acquired using an inexpensive off-the-shelf monochrome charge-coupled device (CCD) camera mounted in place of the central rear-view mirror of the car. The algorithm is implemented on a Visionex Smarteye I, an inexpensive single board image-processing system based on the Texas Instruments Incorporated TMS320C30 digital signal processor. The board has four monochrome video inputs, two monochrome frame grabbers, two image buffers, and an output buffer, all composed of 512×512 pixels with a brightness resolution of 8 bits, and an overlay buffer that can be used to generate 16 color graphics overlays, which, along with the contents of the output buffer, appear on an RGB-Sync video output. The processor runs at 40 MHz with one wait state access to external memory and buffers.

The vision system's on-vehicle accuracy is better than ± 5 cm at a look-ahead distance of approximately 6 m. The measurement update rate is approximately 17 Hz. Results are transmitted to the control computer over an RS-232 serial interface.

The algorithm has also been implemented on an Intel Pentium II computer system with a Matrox Meteor-II frame grabber. This implementation easily provides 30 Hz (the camera frame rate) position updates.

A complete report on the vision-based lane position sensing system can be found in [14].

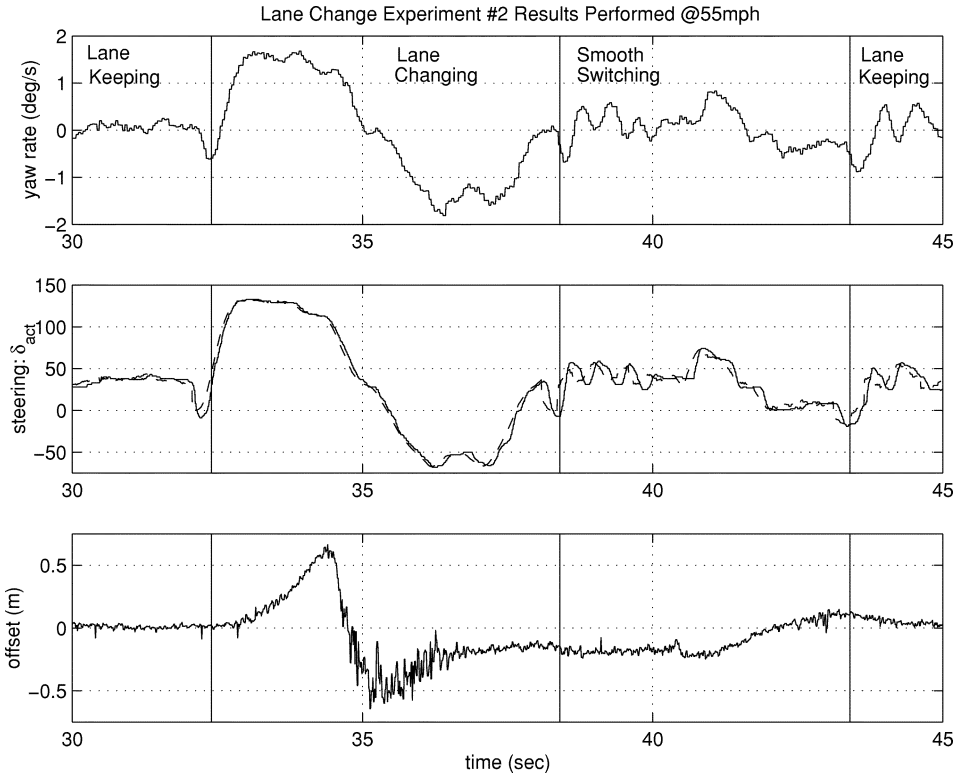

Fig. 8. Experimental results: a right lane change maneuver.

E. Angular Rate Gyroscope

A fiber-optic rate gyro, also supplied by Honda, was used to measure the yaw rate of the vehicle. The angular rate limits are $\pm 60^{\circ}$/s with a sensitivity of 0.01°/s. The sensor is queried by the control computer at a rate of 50 Hz over an RS-232 serial interface.

V. Experimental Results

The experimental data presented here was collected on the I-15 high occupancy vehicle (HOV) lanes north of San Diego, CA. Here, we will focus only on the time when a lane change is being performed. The first set of experimental data, shown in Fig. 7, corresponds to a left lane change at a velocity of 20 m/s (45 mi/h). The lane keeping system uses the radar sensor exclusively while the vision sensor is available as a backup. The second experiment, shown in Fig. 8, is a right lane change performed at 25 m/s (55 mi/h). It corresponds to the completion stage of a double lane change and vehicle passing maneuver in the overall scenario. These plots indicate the time periods during which the lane keeping, lane changing, and smooth switching actions are active. Note that the offset signal during the transition does not provide valid information when it exceeds ± 0.5 m. On the offset signal plots, one can observe that the completion of lane change maneuver leaves the vehicles with a 0.3- and 0.2-m offset from the new lane center. The switching phase, however, steers the vehicle toward the lane center smoothly.

Though the results above show only data collected with vehicle velocities of 45 and 55 mi/h, it should be noted that successful lane keeping and lane changes are obtained at speeds from 10 to 70 mi/h.

VI. Conclusions

This paper summarizes the lane change controller development studies conducted at the Center for Intelligent Transportation Research, Ohio State University, Columbus, and presents the experimental results obtained for road tests performed at San Diego, CA. The design was motivated by the discontinuous availability of valid preview data from the sensing systems during lane-to-lane transitions. The task is accomplished by the generation of a virtual yaw reference and the utilization of a robust switching controller to generate steering commands that cause the vehicle to track that reference. In this way, the open loop lane change problem has been converted into an equivalent virtual reference trajectory tracking problem. Robustness with respect to parameter variations and modeling errors is mentioned; however, the extent of robustness with respect to lateral wind-gust effects are not addressed. The wind can disturb the vehicle's response by effecting its lateral position and its orientation with respect to the road. The pure lateral displacements are mainly contained in the lateral acceleration information that is not measured explicitly. However, its effect on the vehicle orientation will be handled by the sliding mode yaw rate following controller.

References

[1] J. Ackermann, J. Guldner, W. Seinel, R. Steinhauser, and V. I. Utkin, "Linear and nonlinear controller design for robust automatic steering," *IEEE Trans. Contr. Syst. Technol.*, vol. 3, pp. 132–143, Jan. 1995.

[2] W. Chee and M. Tomizuka, "Lane change maneuver of automobiles for the Intelligent Vehicle and Highway Systems (IVHS)," in *Proc. ACC*, vol. 3, Baltimore, MD, 1994, pp. 3586–3587.

[3] ——, "Experimental study of a lane change maneuver for AHS applications," in *Proc. ACC*, vol. 1, Seattle, WA, 1995, pp. 139–143.

[4] C. J. Dixon, *Tires, Suspension and Handling*, ser. SAE R-168. London, U.K.: SAE, 1996.
[5] J. R. Ellis, *Vehicle Dynamics*. London, U.K.: London Business Books Ltd., 1967.
[6] D. Farkas, J. Young, B. Baertlein, and Ü. Özgüner, "Forward-looking radar navigation system for 1997 AHS demonstration," in *Proc. IEEE ITSC Conf.*, Boston, MA, 1997, pp. 672–676.
[7] C. Hatipoglu, "Lateral control of vehicles for highway automation," M.S. thesis, Dept. Elect. Eng., The Ohio State Univ., Columbus, OH, 1995.
[8] C. Hatipoglu, Ü. Özgüner, and K. A. Ünyelioglu, "Advanced automatic lateral control schemes for vehicles on highways," in *Proc. IFAC World Congr.*, vol. Q, San Francisco, CA, 1996, pp. 477–483.
[9] C. Hatipoglu, K. Redmill, and Ü. Özgüner, "Steering and lane change: a working system," in *Proc. IEEE ITSC Conf.*, Boston, MA, 1997, pp. 272–277.
[10] S. Kato, K. Tomita, and S. Tsugawa, "Lane change maneuvers for vision-based vehicle," in *Proc. IEEE ITSC Conf.*, Boston, MA, 1997, pp. 129–134.
[11] Ü. Özgüner, K. A. Ünyelioglu, C. Hatipoglu, and F. Kautz, "Design of a lateral controller for cooperative vehicle systems," SAE, SAE Paper 95(0474) [also (SP-1076)], 1995.
[12] Ü. Özgüner, C. Hatipoglu, A. İftar, and K. Redmill, "Hybrid control design for a three vehicle scenario demonstration using overlapping decompositions," in *Hybrid Systems IV*, ser. LNCS 1273. Berlin, Germany: Springer-Verlag, 1997, pp. 294–328.
[13] Ü. Özgüner, C. Hatipoglu, and K. Redmill, "Autonomy in a restricted world," in *Proc. IEEE ITSC Conf.*, Boston, MA, 1997, pp. 625–630.
[14] K. Redmill, "A simple vision system for lane keeping," in *Proc. IEEE ITSC Conf.*, Boston, MA, 1997, pp. 212–217.
[15] H. S. Tan, J. Guldner, C. Chen, and S. Patwardhan, "Changing lanes on automated highways with look-down reference systems," in *IFAC Advances in Automotive Control Workshop*, Loudonville, OH, 1998, pp. 69–74.
[16] K. A. Ünyelioglu, C. Hatipoglu, and Ü. Özgüner, "Design and stability analysis of a lane following controller," *IEEE Trans. Contr. Syst. Technol.*, vol. 5, pp. 127–134, Jan. 1996.
[17] K. D. Young and Ü. Özgüner, "Sliding-mode design for robust linear optimal control," *Automatica*, vol. 33, no. 7, pp. 1313–1318, 1997.
[18] R. Rajamani, H. S. Tan, B. K. Law, and W. B. Zhang, "Demonstration of integrated longitudinal and lateral control for the operation of automated vehicles in platoons," *IEEE Trans. Contr. Syst. Technol.*, vol. 8, pp. 695–708, July 2000.

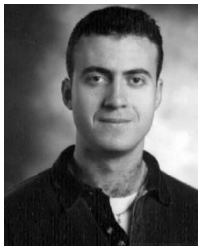

Cem Hatipoglu (S'94–M'98) received the B.S.E.E. and B.S. Phys. degrees from Bogazici University, Istanbul, Turkey, in 1993, the M.S.E.E. and Ph.D. degrees from The Ohio State University, Columbus, in 1995 and 1998, respectively, and the M.B.A. degree from Case Western Reserve University, Cleveland, OH in 2001.

Since 1998, he has been with Bendix Commercial Vehicle Systems LLC (now Honeywell Bendix Commercial Vehicle Systems), Elyria, OH, where he is currently an Automotive Control Systems Engineer. He has authored or coauthored various papers that were featured in IEEE, the Society of Automotive Engineers (SAE), and intelligent transportation systems (ITS) publications. His research interests include advanced automotive control, nonlinear control, variable structure control, system identification, and robust control.

Dr. Hatipoglu is an Associate Member of the SAE. He has served as an associate editor for the IEEE Control Systems Society CEB since 2000.

Ümit Özgüner (S'72–M'75) received the Ph.D. degree from the University of Illinois, Urbana-Champaign, in 1975.

He has held research and teaching positions with the IBM T. J. Watson Research Center, University of Toronto, and Istanbul Technical University, and has spent portions of his sabbaticals with the Ford Motor Company and NASA Lewis Research Center. Since 1981, he has been with The Ohio State University, Columbus, where he is currently a Professor of electrical engineering and holds the TRC Inc. Chair on ITS. His research concerns intelligent control for large-scale systems with applications to automotive control and transportation systems. He led The Ohio State University team effort in the 1997 Automated Highway System demonstration in San Diego, CA. He has authored over 250 publications in journals, books, and conference proceedings.

Prof. Özgüner was president of the IEEE ITS Council in 1999 and 2000 and an elected member of the Control Systems Society Board of Governors. He has participated in organizing many conferences, including serving as the general chair of the 2002 CDC.

Keith A. Redmill (S'90–M'98) received the Ph.D. degree from The Ohio State University, Columbus, in 1998.

He is currently a Senior Research Associate with the Department of Electrical Engineering and the Center for Automotive Research and Intelligent Transportation Systems, The Ohio State University. He has held various teaching and research assignments. He served as the Project Engineer for The Ohio State University autonomous vehicles and automated highway systems project, which participated in the National Automated Highway System Consortium (NAHSC)'s 1997 Technical Feasibility Demonstration, San Diego, CA. He also designed and implemented the image-processing-based lane marker sensing algorithm used for lateral vehicle control. His interests include control and systems theory, autonomous systems and robots, intelligent control, hybrid systems, image processing, embedded real-time systems, global positioning system (GPS) and navigation, sensor technologies, mobile wireless communications, numerical analysis and scientific computation, mathematical modeling, and cognitive science.